Dynamic Reactor Modelling and Operability Analysis of Xylose Dehydration to Furfural Using an Extractive-reaction Process in an Agitated Cell Reactor

Markku Ohenoja*, Pekka Uusitalo*, Fernando Russo Abegão, Abdullahi Adamu**, Kamelia Boodhoo**, Mika Ruusunen***

**Environmental and Chemical Engineering Research Unit, Control Engineering Group, Faculty of Technology, P.O.Box 4300, University of Oulu, Oulu, 90014, Finland (e-mail: markku.ohenoja@oulu.fi).*

*** School of Engineering, Newcastle University, Newcastle upon Tyne, NE1 7RU, United Kingdom*

Abstract: Valorisation hemicellulose into furans chemicals is of great interest to create sustainable furan alternatives to fossil-derived products. A route of particular interest is acid-catalysed dehydration of the hemicellulose pentoses in aqueous medium, with simultaneous extraction of furfural using organic solvent. Agitated Cell Reactor (ACR) could be effectively used to intensify this process and decouple mixing from the long reaction time. This study presents a mathematical model for dehydration of C5 sugars to produce furfural in an ACR. The model can be used to study the effect of feed concentration to the product properties, the concentration profiles along the reactor length, and the dynamic behaviour of the system under feed disturbances or flow rate adjustments. The model was successfully fitted to the experimental data of a laboratory scale ACR for the target product. A simulation study was conducted to analyse the controllability of the process. Operability analysis with the nominal input space and the design space was used for mapping the most feasible region for the process design to meet the flexibility or controllability already at the design phase of the reactor system.

Keywords: Simulation, Controllability, Process intensification, Agitated cell reactor, Furfural.

1. INTRODUCTION

In order to minimise impact on climate change and reduce dependency of non-renewable fossil resources, it is necessary to convert fuels and chemical production to more sustainable synthesis routes using renewable and circular feedstocks, such as biomass. Lignocellulose biomass is the most abundant type of biomass worldwide, being a valuable resource with efficient conversion routes for production of biorenewable chemicals being developed. The biorefining processes being engineered, fractionate lignocellulose into cellulose, hemicellulose and lignin using a range of technologies. The majority of the processes create relatively pure streams of cellulose fibres and/or lignin. However, hemicellulose (HMC), a branched heteropolymer composed mostly of pentoses and some hexose sugars, often ends partially hydrolysed in very diluted aqueous streams, often contaminated with other soluble species such as inorganics, acids and extractives (Wan Azelee et al., 2023). To increase the usage of lignocellulose as a renewable raw material, it is therefore required to be able to convert HMC sugars effectively and overcome the issues associated with diluted streams, and consequent difficulty and cost of separation.

A promising strategy is to dehydrate the HMC sugars into furans using an acid catalyst, where all C5 sugars are converted into furfural (FUR) and all C6 sugars are converted into 5-hydroxymethylfurfural (5-HMF) (Esteban et al., 2020; Ricciardi et al., 2021). This eliminates the need to purify the individual sugars, and creates product convergence, reducing downstream separation requirements. Simultaneously, it produces two high-value platform compounds for fuels and chemicals, with furfural being recently investigated for production of sustainable aviation fuels, and 5-HMF being used in production of renewable monomers (Mariscal et al., 2016).

Nevertheless, due to the diluted nature of the HMC hydrolysates, it is necessary to process these efficiently in aqueous medium, as water cannot be removed without paying a large energy penalty. This creates challenges since furans are reactive intermediates and, in aqueous medium, can easily undergo self-condensation into humins. Additionally, in the case of 5-HMF, it can also decompose by rehydration into levulinic and formic acid (Esteban et al., 2020; Tong et al., 2010).

To improve product yields, process intensification techniques can be employed. In particular, extractive-reaction technology (Trambouze and Piret, 1960) can significantly enhance the yields as it prevents furan decomposition by carrying out *in situ* extraction of the furan products from the aqueous reaction medium using an immiscible organic solvent (Esteban et al., 2020; Ricciardi et al., 2021).

To ensure the mass transfer of furans between the aqueous and organic solvent media is efficient, good mixing is required. Nevertheless, the required reaction times are in the order of several minutes to a couple of hours, and tubular reactors are not able to offer good mixing for such slow flow conditions. Continuous stirred tank reactors (CSTRs) can offer good mixing at longer residence times, but typically operate at low concentrations of reactants and high concentrations of products, with such conditions promoting furan degradation. It

is therefore important to select appropriate reactor technology capable of decoupling mixing from reaction time. A good compromise between good mixing and long residence times is achieved by using a cascade of CSTRs, where the reaction progresses fractionally in each tank, and where there is good mixing in each stage of the cascade. For small scale production and process development, setting a cascade of CSTRs can be costly due to the number of reactors and agitators required, and difficult to control. Alternatively, mixing intensification and decoupling between mixing and residence time can be achieve using an Agitated Cell Reactor (ACR).

The ACR is suitable for both homogeneous and multiphase reactions. In (Toftgaard Pedersen et al., 2017), several applications are listed, where the ACR has been used including continuous processing of slurries (Browne et al., 2011), hydrodechlorination of organic waste (Gómez-Quero et al., 2011), functionalization of carbon nanotubes (Salice et al., 2012), and biocatalytic oxidation reactions (Gasparini et al., 2012; Jones et al., 2012). Specific to the furan production in this work, the ACR is expected to intensify mixing and increase the liquid-liquid interfacial area. Consequently, this will enhance mass transfer rates, allowing the reduction of the amount of extraction solvent used, and resulting in small reaction vessels and lower separation costs downstream. This will also help to control the reaction system selectivity.

To achieve an holistic view on process intensification and a fully integrated process with optimal performance, it is also necessary to account for the process operability, controllability and safety during the conceptual process design (Tian et al., 2018). The operability analysis was casted into process intensification in (Carrasco and Lima, 2017). An operability-based algorithm was presented and used for input–output analysis of nonlinear systems comprising the process intensification goals in the calculation. Furthermore, an optimisation-based approach was applied to determine the feasible operating envelope (desired input set satisfying the design constraints and the desired output set).

This study aims to develop the necessary mathematical tools for optimizing the design of a novel, intensified reactor while taking into account the process operability. Therefore, a dynamic model was developed to simulate the response of the ACR during dehydration of xylose, the most representative sugar in HMC hydrolysate streams produced in biorefining processes. A validation of the model was performed for experimental data representing different feed properties and reactor conditions. The model was then used to analyse the operability of the ACR system for this biorefining application to gain insight on the effect of foreseen process disturbances to the process performance, and thus to support the process design already at the conceptual design phase.

The rest of the article is structured as follows: Section 2 presents the laboratory-scale ACR reactor and the developed dynamic model, as well as the applied methodology for the operability analysis. In Section 3, the model identification and validation are performed. Section 4 presents the case for the operability study, followed by conclusions in Section 5.

2. MATERIALS AND METHODS

2.1 System description

ACRs make use of a reactor block with multiple cylindrical horizontal cells in series, with each cell containing a cylindrical agitator positioned loosely inside. The entire reactor block is then oscillated horizontally, causing the agitators to move freely inside the cells, rolling back and forth and disrupting the flow through each cell. Each cell in the reactor then replicates a CSTR, with the entire reactor block constituting the cascade. Different agitator sizes with different material densities and cylindrical geometries (e.g. solid, hollow tube, coil) can be chosen depending on what is more beneficial for each application.

An ACR with a total volume of 100 mL (10 mL per cell × 10 cells) is modelled. The reactor is fed with an aqueous mixture of xylose and sulphuric acid catalyst and pure MIBK (methyl isobutyl ketone) as the organic solvent for extractive phase.

Five components were considered in the models: xylose (*Xyl*), furfural in aqueous phase (*Faq*), furfural in organic phase (*Forg*), degradation products (*DG*), and intermediate products (*Int*). It is assumed that only furfural would transfer between the aqueous and organic phase, while other components remained in the aqueous phase. The degradation products describe a variety of organic compounds, particularly humins, formed during self-condensation reactions of the xylose, intermediates and furan products. Finally, the intermediate products can be various carbohydrate-based compounds resulting from partial reaction of xylose, and which react further to produce furfural or degradation products.

At the initial state, it is assumed that the entire reactor volume is filled with reactants and MIBK solvent at a volumetric ratio of 1:1, and the operation pressure is achieved. The temperature at which reactions starts is assumed to be 90 °C at t = 0 min, from which point the temperature increases until it reaches the final operation temperature.

The agitation frequency of the ACR is assumed to be fixed at 5 Hz. Thus, the mixing intensity and its effects to the mass transfer are omitted in modelling.

2.2 Model structure

The model structure here consists of a cascade of continuous stirred tank reactors (CSTRs) connected in series with forward flow and an optional backflow term (Roemer and Durbin, 1967). A similar approach for ACR modelling has been proposed in (Toftgaard Pedersen et al., 2017).

The component balances were defined for the mentioned components $C_{i,Xyl}, C_{i,Faq}, C_{i,Forg}, C_{i,Deg}$ and $C_{i,Int}$ in each reactor i resulting in a set of ordinary differential equations (ODEs), represented by (1).

$$\frac{dC_{i,j}}{dt} = r_{i,j} + \frac{v_{aq}}{V_{aq}}\left(C_{i-1,j} - C_{i,j}\right) + \frac{v_B}{V_{aq}}\left(C_{i+1,j} + C_{i-1,j} - 2C_{i,j}\right) \quad (1)$$

In (1), the v_{aq} is the flow rate of aqueous phase, V_{aq} is the volume of aqueous phase in reactor cell, v_B is the backflow rate, and $r_{i,j}$ is the formation or consumption of component j due to reactions or mass transfer between phases. There is no backflow stream leaving from the first unit, thus the term $2C_{i,j} = 0$ for i = 1. Similarly, with the last unit, there is no incoming backflow term from the next unit and the backflow term is $(C_{i-1,j} - C_{i,j})$. For furfural in the organic phase, the flow term in the balance equation uses the flow rate and volume of organic phase (v_{org} and V_{org}, respectively), instead of v_{aq} and V_{aq}. The model was implemented to MATLAB® and a variable-step, variable-order method 'ode15s' was used to solve the ODEs.

2.3 Kinetics for xylose dehydration to furfural

The reaction mechanism is assumed to follow the pathways presented by (Jakob et al., 2022). The studied reaction pathway can be seen in Fig. 1. The reaction rates are first order (2—6) and follow an Arrehenius temperature dependence (7). The acid catalyst concentration (C_{Cat}) is accounted by multiplying the intrinsic reaction rates (k_{x0}) with the ion concentration of H_2SO_4 catalyst (8). The temperature dependency of the dissociation constant K_A and the ion concentration C_{H^+} are calculated as in (9) and (10), respectively (Guo et al., 2021).

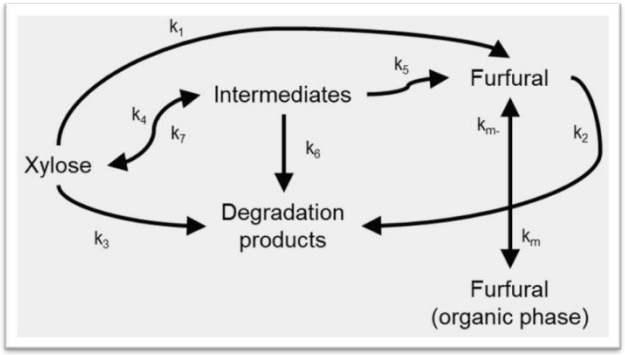

Fig. 1. Reaction mechanism.

In Fig. 1, and Figs. 2 to 6, the k_x are the apparent rate constants, k_m is the mass transfer rate constant for furfural from aqueous phase to organic phase, and k_{m-} is the mass transfer rate constant for furfural from organic phase to aqueous phase. T is the operation temperature and T_{ref} the reference temperature, $E_{a,x0}$ the activation energy and R is he ideal gas constant.

$$r_{i.Xyl} = -k_1 C_{i.Xyl} - k_3 C_{i.Xyl} - k_4 C_{i.Xyl} + k_7 C_{i.Int} \quad (2)$$

$$r_{i.Faq} = k_1 C_{i.Xyl} - k_2 C_{i.Faq} + k_5 C_{i.Int} - k_m C_{i.Faq} + k_{m-} C_{i.Forg} \quad (3)$$

$$r_{i.Forg} = k_m C_{i.Faq} - k_{m-} C_{i.Forg} \quad (4)$$

$$r_{i.Deg} = k_3 C_{i.Xyl} + k_2 C_{i.Faq} + k_6 C_{i.Int} \quad (5)$$

$$r_{i.Int} = k_4 C_{i.Xyl} - k_7 C_{i.Int} - k_5 C_{i.Int} - k_6 C_{i.Int} \quad (6)$$

$$k_{x0}(T) = k_{x0}(T_{ref}) exp \frac{E_{a,x0}}{R} \left(\frac{1}{T_{ref}} - \frac{1}{T}\right) \quad (7)$$

$$k_x = C_{H^+} \times k_{x0} \quad (8)$$

$$K_A = \exp\left(0.0152 \times T + 2.636\right) \quad (9)$$

$$C_{H^+} = C_{Cat} + \frac{1}{2}\left(-K_A - C_{Cat} + \sqrt{(K_A + C_{Cat})^2 + 4 C_{Cat} K_A}\right) \quad (10)$$

The rate constants and activation energies are given in (Jakob et al., 2024). In addition, the mass transfer coefficient value and partition coefficient value were based on (Weingarten et al., 2010).

2.4 Intensification factor and temperature profile

In order to simulate the intensified reactor with improved mixing, and thus mass transfer, an intensification factor F was applied to the model. For simplificity, a single lumped value was assumed that multiplies the rate constants and the forward mass transfer constant, as in (11). The value for F was estimated using the experimental data.

In addition to the intensification factor, the model fitting comprises an unknown, transient temperature profile for the reactor start-up. The temperature increment to the target operation temperature was assumed to follow an exponential function seen in (12). The value for time constant h was estimated using experimental data.

$$k_{intensified} = k_x \times F \quad (11)$$

$$T(t) = T(0) - \big(T(t) - T(0)\big) \exp\left(-h \times t\right) \quad (12)$$

2.5 Operability analysis

Process operability analysis focuses on evaluating in what extent the desired process outputs (controlled variables, desired output space) can be achieved with the assumed range of input variables (manipulated variables, available input space) and expected disturbances. The analysis does not assume any specific control structure. The same analysis can also be conducted to evaluate whether the process design satisfy the desired intensification targets and constraints (Carrasco and Lima, 2017).

An open-source MATLAB® tool 'Operability App' was applied for the operability study in this work. The operability index (*OI*) for a design region is used to evaluate the feasible process design in terms of operability. *OI* calculation uses the desired outputs set (*DOS*) and achievable output set (*AOS*) divided into subregions and applies computational geometry tools to determine the ratio of achieved *DOS* subregions and the total number of *DOS* subregions (13).

$$OI = \frac{\mu(AOS \cap DOS)}{\mu(DOS)} \quad (13)$$

AOS is the set of controlled variables that the process design can achieve for the available input set (operational and design variable space) and disturbance set. Process model is used to

describe the process behaviour and, thus, to define *AOS*. The applicability of the software tool for process achievability analysis, intensification, and modularization has been demonstrated in (Gazzaneo et al., 2020) and (Gazzaneo, 2021), where also further details of the method can be found.

3. MODEL IDENTIFICATION AND VALIDATION

3.1 Model fitting

The model performance was qualitatively evaluated against the experimental data acquired from a synthetic feed stream with xylose monosaccharides as a starting compound. The feed concentration was 42.3 g/L, operation temperature at 125 °C, and catalyst concentration 0.2 M. The volumetric ratio of the phases was 1:1. The feed rates of both phases are calculated based on the target residence time of aqueous phase in the reactor. The nominal residence time is 120 min, corresponding a feed rate of 0.42 mL/min of both phases.

The model was simulated with different values of F and h. Figure 2 presents the fitted concentration values at the reactor exit with $F = 12$ and $h = 0.015$ min^{-1}. It can be seen that the xylose consumption and total furfural formation are in a good agreement between the model and experimental data. The experimental results for furfural in aqueous phase show very small concentrations (<0.2 g/L). However, the simulation shows higher concentration of furfural in aqueous phase comparatively to the experiment. This implies that the mass transfer of furfural from aqueous phase to organic phase is underestimated in the model.

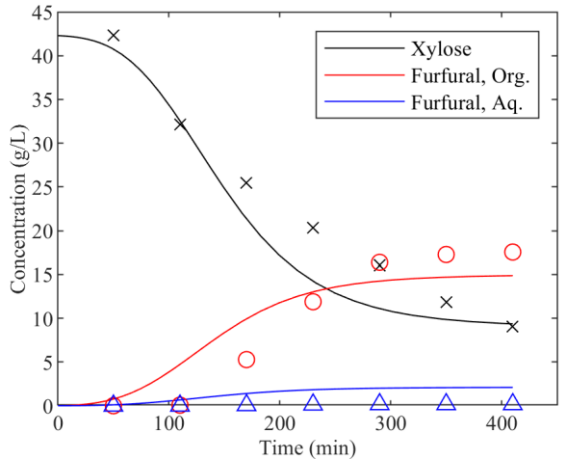

Fig. 2. Evolution of concentration as a function of time. Lines represent the simulation. Tick marks represent the experimental data.

3.2 Transfer to real hemicellulose streams

The model input parameters ($C_{1,Xyl}$, T, v_{aq}, v_{org}, C_{Cat}) were then changed to represent three other experimental cases: one with the same synthetic stream but a different residence time, and two experimental campaigns with real HMC streams.

In Table 1, the error between the predicted and experimental total furfural concentrations (organic + aqueous) at steady-state for the four experimental data sets are shown, when the simulations were run with fixed values of F and h. As expected, the error is higher for the three cases, where the model was extrapolated to. For the synthetic stream with lower residence time (RT), the model overestimates the furfural concentration. For the first real HMC stream, the direction of the modelling error is the same. However, for the second real HMC stream, the model slightly underestimated the furfural concentration. Taking into account the complexity of the modelled system and simplicity of the fitting approaches, the proposed modelling approach was effective and provided acceptable results with respect to the target compound furfural.

Table 1. Error in steady-state furfural concentration.

Case	Absolute error	Relative error
Synthetic, RT=120 min	−0.77 g/L	−4.3 %
Synthetic, RT=60 min	2.75 g/L	36.8 %
Real HMC #1	2.22 g/L	25.2 %
Real HMC #2	−1.46 g/L	−10.6 %

3.3 Implications

Sugar dehydration reactions are complex networks (Dussan et al., 2015), making analysis of hemicellulose streams dehydration challenging due to the wide range of sugars present. Moreover, it is often difficult to find available kinetic data for all sugars using the same catalyst, reactor type (which can mask mixing, mass transfer and other limitations) and process conditions. Nevertheless, the high potential for valorisation of these streams, and the appeal of using dehydration reactions as a route to product convergence and reduction of downstream processing requirements, highlights the importance of developing the understanding of these systems and be able to simulate them in simple and effective ways.

The models developed demonstrate that transferability of kinetic data between batch and intensified flow reactor systems is possible by employing a simple Intensification Factor, whilst still retaining the overall system behaviour, and providing practical tools to model the system dynamic behaviour of intensified ACRs. This is expected to notably speed up modelling, design and preliminary optimisation calculations, contributing to the overall sustainability of the biorefinery.

When looking at the concentration values at the reactor exit for the real HMC stream #1, depicted in Fig. 3, the modelled predictions for xylose concentration deviate remarkably from the experimental observations. The model suggests that the concentration of monosaccharide xylose should evolve to substantially lower values than what was observed in the experiments. There is indeed a natural explanation to this model-data mismatch: the real HMC streams can contain a significant amount of oligosaccharides that undergo hydrolysis to the corresponding monosaccharides at similar reaction conditions. Therefore, while some of the xylose is converted, some more monomeric xylose is formed. Thus, for HMC hydrolysate stream where the amount of oligomers is

significant, oligomers hydrolysis should also be accounted for in future model developments, incorporating literature hydrolysis kinetic models and validation against experimentation which includes analysis of oligomers concentration over time.

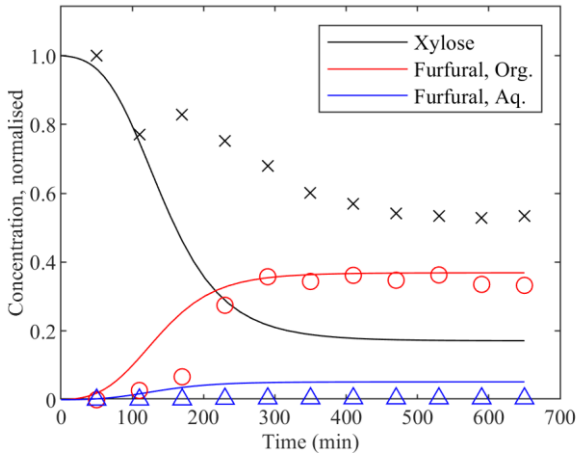

Fig. 3. Concentration (normalised) as a function of time for real HMC stream. Lines represent the simulation. Tick marks represent the experimental data.

4. OPERABILITY STUDY

4.1 Simulation scenario

Due to the heterogeneity of the biomass properties, and the disturbances in upstream processes, the concentration of xylose in the feed stream has natural variability. In the operability study, a simulation scenario is built, where different transients take place during the continuous processing. Namely, it is assumed that the feed concentration is subject to a sudden +25% change after the first steady-state is reached. After that, a second change takes place with -25% xylose concentration with respect to the nominal value. Again, after the steady-state, a third change occur with the feed concentration returning its nominal value.

The desired output space is determined by two process performance variables dependent on the dynamic performance of the system; The cumulative amount furfural production (y_1) and the cumulative amount of degradation and intermediate products (y_2) during the simulated period. The rationale for the first is obvious, as furfural is the target product. For the second output variable, production should be minimized in order to avoid excessive carbon (*e.g.* humins) formation that can possibly lead to reactor fouling. The ranges are given in Table 2.

The available input space is also presented in Table 2. For the design variables, the reactor size ($u_{des,1}$) and the catalyst loading ($u_{des,2}$) are used as available inputs. The volume of ACR reactor can be altered by changing the mixing elements. The operational inputs are assumed to be the aqueous phase feed flow rate ($u_{op,1}$) and the feed ratio of aqueous and organic phases ($u_{op,2}$). Higher value for the feed ratio corresponds to larger volume of reacting phase (aqueous) in the reactor.

Table 2. Variable ranges in the operability study.

	Nominal	Minimum	Maximum
$u_{des,1}$ (mL)	100	60	100
$u_{des,2}$ (mol/L)	0.2	0.1	0.3
$u_{op,1}$ (mL/min)	0.42	0.30	0.60
$u_{op,2}$ (-)	0.5	0.4	0.6
y_1 (kmol)		6	10
y_2 (kmol)		0	2

4.2 Results

For the nominal process design, Figure 4 presents the furfural production rate at the reactor exit as a function of time, when a 25% stepwise increment in xylose feed concentration takes place at t=0. It can be seen that the due to the long residence time, the new steady-state is achieved after a period of 216 min (2% settling time). Naturally, this prevents establishing an efficient feedback control of ACR system with the studied reactions and a careful design of the system is needed to establish feedforward control for feed disturbances entering the system.

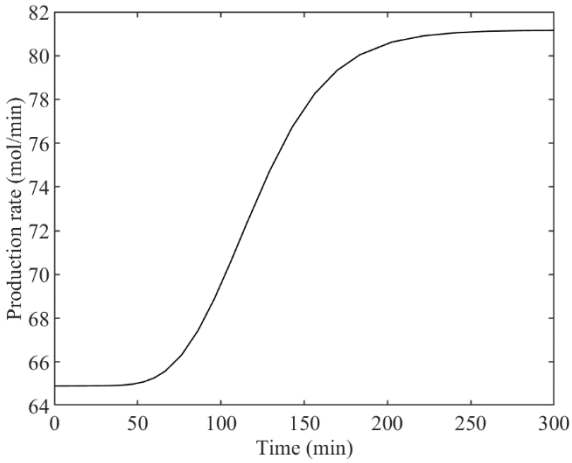

Fig. 4. Simulated dynamic response of the furfural production in nominal conditions to +25% increment of xylose feed at 0 min.

OI for a design region was evaluated for nine different process design ($u_{des,1}$, $u_{des,2}$), as presented in Table 3. *OI* is a scalar number describing the proportion of subregions in the desired output space that can be achieved with the available operational inputs in each process design. From Table 3, it can be seen that the process design with reactor size ($u_{des,1}$) of 80 mL and catalyst concentration of 0.2 mol/L shows the best operability (*OI* = 67%).

Each design can also be interpreted with the achievable output space, as depicted in Fig. 5. There, the desired output space is given as the light grey shaded area divided into nine subregions. Three examples of process designs are given and illustrated as the dark grey polyhedrons. Design 4 shows a

narrow range of obtained outputs, which all lie outside the desired output space. Thus, also *OI* is equal to zero (see Table 3). This is due to the combination of limited residence time and low catalyst concentration, contributing to moderate production of both the target furfural and the degradation products.

Table 3. Operability indices for the different designs.

Design	$u_{des,1}$	$u_{des,2}$	*OI*
1	60	0.1	0
2	60	0.2	22
3	60	0.3	56
4	80	0.1	0
5	80	0.2	67
6	80	0.3	33
7	100	0.1	11
8	100	0.2	33
9	100	0.3	33

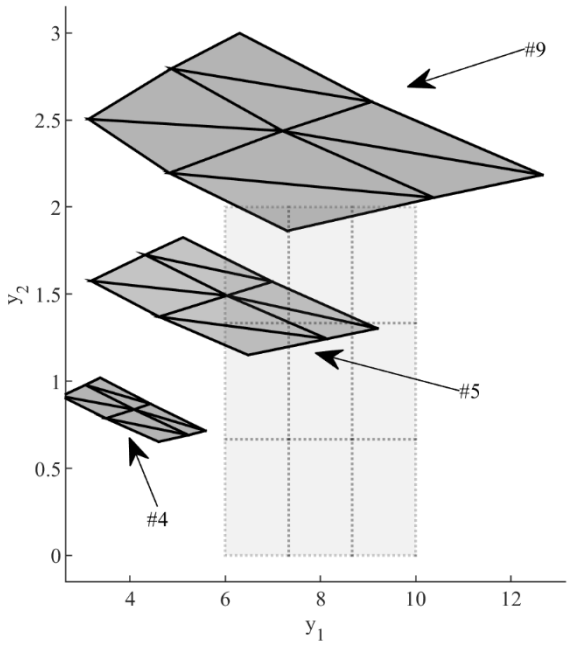

Fig. 5. Achievable output space (represented by the dark grey areas) for designs 4, 5 and 9. The desired output space is given in light grey colour.

Design 9 suggests that the system can achieve cumulative furfural production (y_1) under feed disturbances up to 12.7 kmol. However, this design also contributes to substantial degradation product formation, thus most of the operational space lying outside the desired region. According to Table 3, the design 9 can achieve 33% of the design space, but Figure 5 reveals that only small part of those design regions can be reached with this input space. Finally, design 5 seems to have the highest *OI* (67%) as it can reach at least a small portion of six different regions in the desired output space. This process design shows the best performance in terms of operability.

4.3 Implications

In comparison, a different process design optimisation target could be based on the xylose conversion and furfural yield (to the organic phase) in steady-state conditions. By looking at the simulation results from the operability study, the maximum conversion (96.9%) would be attained for the process design with maximal residence time, i.e. $u_{des,1}$ = 100 mL and $u_{op,1}$ = 0.3 mL/min, with $u_{des,2}$ = 0.3 and $u_{op,2}$ = 0.6. Also, yield is preferred by long residence time, with maximum (60.0%) seen in $u_{des,1}$ = 100 mL, $u_{op,1}$ = 0.45 mL/min, $u_{des,2}$ = 0.3 and $u_{op,2}$ = 0.6.

However, with respect to y_1 and y_2, these designs and operation conditions would provide dynamic behaviour (y_1: 3.13 and 4.87 kmol) and excessive degradation products formation (y_2: 2.51 and 2.79 kmol) outside the expected output range of the operability study. This example highlights the need of dynamic analysis and incorporation of dynamic performance as a part of process design, especially in processes where considerable feed disturbances cannot be avoided, or the process dynamics are slow mitigating the feedback control possibilities.

From the operability analysis results, it can be observed that the desired output space is somewhat optimistic, and most of the process states cannot be achieved by changing the selected design and operational variables. The degradation product formation and furfural production are affected to the same direction by the different inputs, and thus the degradation product formation cannot be pushed down without negative effect on the furfural production.

The operability could be improved by allowing larger ranges for the operational inputs. However, as both inputs affect the residence time of reaction phase, the extension of ranges can have a competing effect to the residence time. There are also limits with the ratio (y_2) as both phases need to flow through the reactor, and the high amount of organic phase would result in higher capacity demand for the downstream separation steps of furfural and MIBK.

As a future work, the model should be developed to comprise also the temperature balance. This would allow to simulate the operation temperature as an operational input and use in control design to compensate the feed variations. Temperature balance would also allow more accurate predictions of concentrations along the reactor length as the temperature gradient affect to the reactions rates, ion concentration, and mass transfer coefficients. Addition of catalyst mass balance would also establish using the catalyst concentration as an operational variable instead of (fixed) design variable.

Finally, the operability analysis could also involve the ACR mixing intensity as an input. This has been modelled for example in (Miller, 2021), where its effect to the mass transfer was studied. The mixing intensity can then be linked to the furfural mass transfer between the phases, and to the

intensification factor coefficient. However, additional experimental work would be needed to identify these interactions.

5. CONCLUSIONS

Mathematical model aiming to describe the xylose dehydration to furfural using an extractive-reaction process in an agitated cell reactor was presented. A lumped intensification factor was found useful to transfer the kinetic data between batch and intensified flow reactor systems. The proposed modelling approach was effective and provided acceptable validation to experimental data. Operability of the ACR system was studied with the model. The demonstration highlighted how most of the process states cannot be achieved by changing the selected design and operational variables within their ranges. Instead, the desired output space needs to be reconsidered. This implies that the operability measures should be seen as inputs already at the conceptual process design.

ACKNOWLEDGEMENTS

This project has received funding from the Bio-based Industries Joint Undertaking (JU) under the European Union's Horizon 2020 research and innovation programme under grant agreement No 887226. The JU receives support from the European Union's Horizon 2020 research and innovation programme and the Bio-based Industries Consortium.

REFERENCES

Browne, D. L., Deadman, B. J., Ashe, R., Baxendale, I. R., and Ley, S. V. (2011). Continuous Flow Processing of Slurries: Evaluation of an Agitated Cell Reactor. *Organic Process Research & Development*, *15*(3), 693–697. doi: 10.1021/op2000223

Carrasco, J. C., and Lima, F. V. (2017). Novel operability-based approach for process design and intensification: Application to a membrane reactor for direct methane aromatization. *AIChE Journal*, *63*(3), 975–983. doi: 10.1002/aic.15439

Dussan, K., Girisuta, B., Lopes, M., Leahy, J. J., and Hayes, M. H. B. (2015). Conversion of Hemicellulose Sugars Catalyzed by Formic Acid: Kinetics of the Dehydration of D-Xylose, L-Arabinose, and D-Glucose. *ChemSusChem*, *8*(8), 1411–1428. doi: 10.1002/cssc.201403328

Esteban, J., Vorholt, A. J., and Leitner, W. (2020). An overview of the biphasic dehydration of sugars to 5-hydroxymethylfurfural and furfural: A rational selection of solvents using COSMO-RS and selection guides. *Green Chemistry*, *22*(7), 2097–2128. doi: 10.1039/C9GC04208C

Gasparini, G., Archer, I., Jones, E., and Ashe, R. (2012). Scaling Up Biocatalysis Reactions in Flow Reactors. *Organic Process Research & Development*, *16*(5), 1013–1016. doi: 10.1021/op2003612

Gazzaneo, V. (2021). Multimodel Operability Framework for Design of Modular and Intensified Energy Systems. *Graduate Theses, Dissertations, and Problem Reports, West Virginia University,* 8069. doi: 10.33915/etd.8069

Gazzaneo, V., Carrasco, J. C., Vinson, D. R., and Lima, F. V. (2020). Process Operability Algorithms: Past, Present, and Future Developments. *Industrial & Engineering Chemistry Research*, *59*(6), 2457–2470. doi: 10.1021/acs.iecr.9b05181

Gómez-Quero, S., Cárdenas-Lizana, F., and Keane, M. A. (2011). Liquid phase catalytic hydrodechlorination of 2,4-dichlorophenol over Pd/Al2O3: Batch vs. continuous operation. *Chemical Engineering Journal*, *166*(3), 1044–1051. doi: 10.1016/j.cej.2010.07.032

Guo, W., Zhang, Z., Hacking, J., Heeres, H. J., and Yue, J. (2021). Selective fructose dehydration to 5-hydroxymethylfurfural from a fructose-glucose mixture over a sulfuric acid catalyst in a biphasic system: Experimental study and kinetic modelling. *Chemical Engineering Journal*, *409*, 128182. doi: 10.1016/j.cej.2020.128182

Jakob, A., Likozar, B., and Grilc, M. (2022). Aqueous conversion of monosaccharides to furans: Were we wrong all along to use catalysts? *Green Chemistry*, *24*(21), 8523–8537. doi: 10.1039/D2GC02736D

Jakob, A., Likozar, B., and Grilc, M. (2024). Model-assisted optimization of xylose, arabinose, glucose, mannose, galactose and real hemicellulose streams dehydration to (hydroxymethyl)furfural and levulinic acid. *ChemSusChem, Accepted*. doi: 10.1002/cssc.202400962

Jones, E., McClean, K., Housden, S., Gasparini, G., and Archer, I. (2012). Biocatalytic oxidase: Batch to continuous. *Chemical Engineering Research and Design*, *90*(6), 726–731. doi: 10.1016/j.cherd.2012.01.018

Mariscal, R., Maireles-Torres, P., Ojeda, M., Sádaba, I., and Granados, M. L. (2016). Furfural: A renewable and versatile platform molecule for the synthesis of chemicals and fuels. *Energy & Environmental Science*, *9*(4), 1144–1189. doi: 10.1039/C5EE02666K

Miller, J. M. J. (2021). *Solvent Extraction and Mass Transfer Assessment in Novel Extraction Technologies,* Phd thesis, University of Leeds. https://etheses.whiterose.ac.uk/29223/

Ricciardi, L., Verboom, W., Lange, J.-P., and Huskens, J. (2021). Production of furans from C5 and C6 sugars in the presence of polar organic solvents. *Sustainable Energy & Fuels*, *6*(1), 11–28. doi: 10.1039/D1SE01572A

Roemer, M. H., and Durbin, L. D. (1967). Transient Response and Moments Analysis of Backflow Cell Model for Flow Systems with Longitudinal Mixing. *Industrial &*

Engineering Chemistry Fundamentals, *6*(1), 120–129. doi: 10.1021/i160021a021

Salice, P., Fenaroli, D., De Filippo, C., Menna, E., Gasparini, G., and Maggini, M. (2012). Efficient functionalization of carbon nanotubes: An opportunity enabled by flow chemistry. *Chimica Oggi*, *30*, 37–39.

Tian, Y., Demirel, S. E., Hasan, M. M. F., and Pistikopoulos, E. N. (2018). An overview of process systems engineering approaches for process intensification: State of the art. *Chemical Engineering and Processing - Process Intensification*, *133*, 160–210. doi: 10.1016/j.cep.2018.07.014

Toftgaard Pedersen, A., de Carvalho, T. M., Sutherland, E., Rehn, G., Ashe, R., and Woodley, J. M. (2017). Characterization of a continuous agitated cell reactor for oxygen dependent biocatalysis: Biocatalytic Oxidation in a Continuous Agitated Cell Reactor. *Biotechnology and Bioengineering*, *114*(6), 1222–1230. doi: 10.1002/bit.26267

Tong, X., Ma, Y., and Li, Y. (2010). Biomass into chemicals: Conversion of sugars to furan derivatives by catalytic processes. *Applied Catalysis A: General*, *385*(1), 1–13. doi: 10.1016/j.apcata.2010.06.049

Trambouze, P. J., and Piret, E. L. (1960). Extractive reaction: Batch- and continuous-flow chemical-reaction systems, concentrated case. *AIChE Journal*, *6*(4), 574–578. doi: 10.1002/aic.690060414

Wan Azelee, N. I., Mahdi, H. I., Cheng, Y.-S., Nordin, N., Illias, R. M., Rahman, R. A., Shaarani, S. M., Bhatt, P., Yadav, S., Chang, S. W., Ravindran, B., and Ashokkumar, V. (2023). Biomass degradation: Challenges and strategies in extraction and fractionation of hemicellulose. *Fuel*, *339*, 126982. doi: 10.1016/j.fuel.2022.126982

Weingarten, R., Cho, J., Conner, J., Wm. Curtis, and Huber, G. W. (2010). Kinetics of furfural production by dehydration of xylose in a biphasic reactor with microwave heating. *Green Chemistry : An International Journal and Green Chemistry Resource : GC*, *12*(8), Article 8. doi: 10.1039/c003459b